Gokarneshan et al., J Fashion Technol Textile Eng 2015, 3:2
http://dx.doi.org/10.4172/2329-9568.1000121

Journal of Fashion Technology & Textile Engineering

Review Article

A SCITECHNOL JOURNAL

Characterization Methods of Nano Textile Materials

Gokarneshan N*, Gopalakrishnan PP and Anitha Rachel D

Abstract

Nano materials are being used in textile finishing to impart functional properties to the fabrics. This paper deals with the characterization aspect of important nano materials used in textile finishing, viz., titanium dioxide, silver oxide and zinc oxide. Each type of nano material produces its own distinct effect on the fabrics so treated. Various techniques are being used for characterizing the nano particles. These are discussed in detail in this paper. The characterization techniques enable to study the surface characteristics of treated fabrics and also measure the nano particle size.

Keywords: Characterization; Nano particles; Silver oxide' Titanium dioxide; Zinc oxide

Introduction

Nano plastic and nanostructured materials are attracting a great deal of attention of the textile and polymer researchers and industrialists because of their potential applications for achieving specific processes and properties, especially for functional and high performance textile applications [1]. This paper deals with the characterization methods of the important nano materials used in textile finishing. The important nano materials include silver oxide, zinc oxide and titanium dioxide. Silver oxide is well known to imparting antimicrobial properties to the fabrics so treated. Zinc oxide is known for UV protection for fabrics, and titanium dioxide is used for wrinkle resistance. Besides these basic properties, the various nano materials are also used to impart other functional properties. The techniques used are uv absorption spectroscopy, FTIR spectroscopy, and X-ray diffraction, and scanning electron microscopy (SEM) studies. The SEM technique has been used for the investigation of textile materials [2-5]. It can also be used to view dispersion of nano particles such as carbon nanotubes, nanoclays, and hybrid POSS Nanofillers in the bulk and on the surface of nano composite fibres and coatings on yarns and fabric samples [6,7]. The uv absorption spectroscopy has been used to evaluate the uv shielding effectiveness of fabrics. FTIR spectroscopy has been used to evaluate the chemical composition of nano particles and X-ray diffraction is used to evaluate the crystallinity of nano particles.

Characterization of Silver Oxide Nano Particles

Recent studies have shown that silver nanoparticles with less than 50nm size, which are normally used for textile finishing can cause toxic effects on human health and environment [8,9]. Hence it is necessary to produce silver nano particles of > 50nm size for textile applications. In one of the method described, the presence of silver in nano meter size has been qualitatively confirmed by the use of shimadzu UV 1601 spectrometer. An absorption peak ranging in wave length between 400-440 nm could be produced by silver having a nano meter size. The concentration of silver in the synthesized powder has been analyzed using atomic absorption spectrum with Varian spectra 220. The size of the silver nano particles in the nano powder has been determined by means of transmission electron microscope (TEM) analysis using Philips CM 200 model machine by drop coating method. The nano powder was dissolved in the water and drop coated on the copper grids for TEM analysis. The transmission electron microscope has been attached with energy dispersive analysis of X-rays device so as to enable elemental analysis on the individual nano particles [10].

UV Spectra

In the case of Ultraviolet (UV) Spectroscopy, a reference beam in the spectrometer travels from the light source to the detector without interacting with the sample. The sample beam interacts with the sample exposing it to ultraviolet light of continuously changing wavelength. When the emitted wavelength corresponds to the energy level which promotes an electron to a higher molecular orbital, energy is absorbed. The detector records the ratio between reference and sample beam intensities. The computer determines at what wavelength the sample absorbed a large amount of ultraviolet light by scanning for the largest gap between two the two beams. When a large gap between intensities is found, where the sample beam intensity is significantly weaker than the reference beam, the computer plots this wavelength as having the highest ultraviolet light absorbance when it prepares the ultra violet absorbance spectrum. In certain metals, such as silver and gold, the Plasmon resonance is responsible for their unique and remarkable optical phenomena. Metallic (silver or gold) nano particles, typically 40-100 nm in diameter, scatter optical light elastically with remarkable efficiency because of a collective resonance of the conduction electrons in the metal known as surface Plasmon resonance. The surface plasma resonance peak in UV absorption spectra is shown by these plasmon resonant particles. The magnitude, peak wave length, and spectral bandwidth of the Plasmon resonance associated with a nano particle are dependent on the particle's size, shape and material composition as well as the local environment. Besides biological labeling and nanoscale biosensing silver nano particles have received considerable attention to the textile and polymer researchers due to their attractive anti microbial properties. The surface Plasmon resonance peak in absorption spectra of silver particles is shown by absorption of maximum at 420-500 nm. The surface peaks vary with size, shape and concentration of the metallic nano particles. Figure 1 shows how the value of absorbance is shifted towards higher wavelengths with increasing Ag content in a silver nano particle/kaolinite composites. It is reported that the truncated triangular silver nano particles with a lattice plane as the basal plane displayed the strongest biocidal action compared with spherical, rod shaped nanoparticles or with Ag^+ (in the form of

***Corresponding author:** Dr. N. Gokarneshan, NIFT TEA College of knitwear fashion, Tirupur 641 606, India, Tel: 0421 237 4200; E-mail: advaitcbe@rediffmail.com

Received: April 11, 2015 **Accepted:** February 23, 2015 **Published:** February 27, 2015

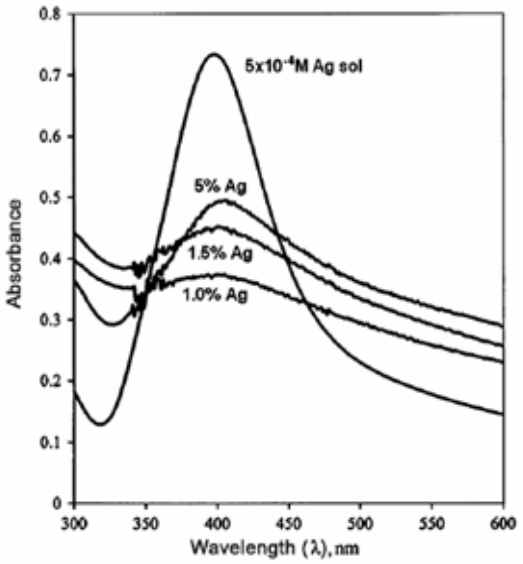

Figure 1: UV absorption spectrum of 5x10^{-4} M and spectra of Ag solution and spectra of suspensions of Ag/Kaolinite samples at different silver contents [11] electrons in a metal.

$AgNO_3$) [11] This shape of silver nanoparticles can be identified by observing the corresponding peak. TEM images of the corresponding particle are shown above their respective spectrum. This example is a representative of the principle conclusion that the peak shifts as per the particle shape and the triangular shaped particles appear mostly red, particles that form the pentagon appear green and the blue particles are spherical.

The optical absorption spectra of metal nano particles shift to longer wavelengths with increasing particle size, the position and shape of th Plasmon absorption of silver nano particles are strongly dependent on the particle size, dielectric medium, and surface adsorbed species [12,13]. According to mis's theory, only a single surface Plasmon resonance (SPR) band is expected in the absorption spectra of spherical nanoparticles, whereas anisotropic particles could give rise to two or more SPR bands depending on the shape of the particles. The number of SPR peaks increases as the symmetry of the nano particle decreases [14]. Thus spherical nano particles, circular disks and triangular nano plates of silver show one, two and more peaks respectively.

The UV-Visible spectra of the produced Polyvinylpyrrolidone coated silver nano particles in both powder and solution form are shown in Figure 2. A clear absorption peak at a wave length of 430 nm has been observed for the spectra obtained in both solution and powder forms, owing to the presence of silver nano particles [15]. The UV-visible spectroscopy is an established method for the confirmation of formation of silver nano particles in solution. An intense absorption peak is produced at 400 nm, by the silver nano particles, which arises from surface Plasmon excitation. Surface Plasmon excitation describes the collective excitation of the conduction electrons in a metal.

TEM and EDAX studies

Transmission electron microscopy (TEM) is a microscopy technique whereby a beam of electrons is transmitted through an ultra thin specimen and interacts as it passes through the sample. An image is formed from the electrons transmitted through the specimen, magnified and focused by an objective lens and appears on an imaging screen. The sample interacts with the electron beam mostly by diffraction rather than by absorption. The intensity of diffraction depends on the orientation of the planes of atoms in a crystal relative to the electron beam. At certain angles the electron beam is diffracted strongly from the axis of the incoming beam, while at other angles the beam is largely transmitted. Modern TEMs are equipped with specimen holders that allow to tilt the specimen to a range of angles in order to obtain specific diffraction conditions. Therefore, a high contrast image can be formed by blocking electrons deflected away from the optical axis of the microscope by placing the aperture to allow only unscattered electrons through. This produces a variation in the electron intensity that reveals information on the crystal structure. The specimens must be prepared as a thin foil so that the electron beam can penetrate. Materials that have dimensions small enough to be electron transparent, such as powders or nano tubes, can be quickly produced by the deposition of a dilute sample containing the specimen onto support grids. As polymeric nano composites or the textile samples are not as hard as metals, they are cut into thin films (<100 nm) using ultra- microtome with diamond knife at cryogenic condition (in liquid nitrogen).

The TEM is used widely both in material science/metallurgy and biological sciences. In both cases the specimens must be very thin and able to withstand the high vacuum present inside the instrument. For biological specimens, the maximum specimen thickness is roughly 1 micrometer. To withstand the instrument vacuum, biological specimens are typically held at liquid nitrogen temperatures after embedding in vitreous ice, or fixated using a negative staining material such as uranyl acetate or by plastic embedding.

The properties of nano composites depend to a large extent on successful nano level dispersion or intercalation/ exfoliation of nano clays, therefore monitoring their morphology and dispersion is very crucial [16]. TEM images reveal the distribution and dispersion of nano particles in polymer matrices of nano composite fibres, nano coatings etc. the extent of exfoliation, intercalation and orientation of nano particles can also be visualized using the TEM micrograph (Figure 3).

Energy Dispersive X-ray (EDX) analysis is a technique to analyze near surface elements and estimate their proportion at different position, thus giving an overall mapping of the sample. It is used in

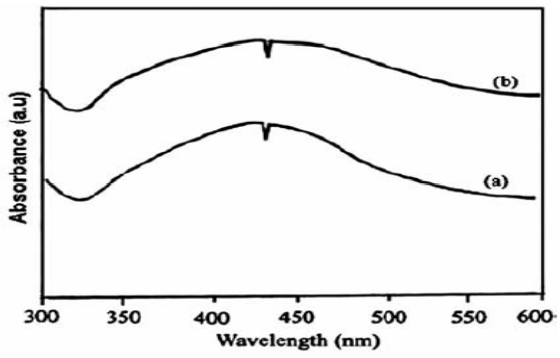

Figure 2: UV visible Spectra of PVP coated silver (a) nano particles in solution (b) nano powder [15].

conjunction with scanning electron microscope an electron beam strikes the surface of a conducting sample. The energy of the beam is typically in the range of 10-20 ekV. This causes X-rays to be emitted from the material. The energy of the X-rays emitted depends on the material under examination. The X-rays are generated in a region about 2 microns in depth, and thus EDX is not truly a surface science technique. By moving the electron beam across the material an image of each element in the sample can be obtained. Due to the low X-ray intensity, images usually take a number of hours to acquire. The composition or the amount of nanoparticles near and at the surface can be estimated using the EDX, provided they contain some heavy metal ions. For example, the presence of gold, palladium, and silver nano particles on surface can easily be identified using EDX technique. Elements of low atomic number are difficult to detect by EDX. The Si-Li detector protected by a beryllium window cannot detect elements below atomic number of 11. In windowless systems, the elements with as low atomic number as 4, can be detected. EDX spectra have to be taken by focusing the beam at different regions of the same sample to verify spatially uniform composition of the bimetallic materials. The incorporation of silver nano particles on cotton cloth can be verified by EDX [17,18].

The TEM image of PVP Coated silver nano particles is shown in Figure 3. The silver nano particles ranged in size between 50 -60nm. As can be observed from the Figure 3, there appear a few big agglomerates of nano particles having size range between 100-200nm [15]. This could be attributed to the thermal migration of nano particles during the drying process in the spray dryer. EDAX has been used for analyzing the various sizes of nano particles presented by TEM image. Figure 4a shows the spectrum at a place having no nano particles, while Figures 4b-d indicates the places having nano particles with sizes of 55, 100 and 200 nm respectively. All the four spectra confirm the presence of Silver nano particles in the synthesized powder. The low intensity peak pertaining to silver in the first spectra is attributed to the presence of silver traces in the polymer matrix. The peak related to copper in all the spectra is due to the use of copper grids in TEM analysis.

Characterization of Zinc Oxide Nano Particles

UV absorption properties

Zinc oxide nano particles have been used for imparting antibacterial and UV blocking properties [19-21]. Besides, they are also unique in their photo-catalytic, electrical, electronic, optical, and dermatological properties [22-28]. The UV-screen properties of the

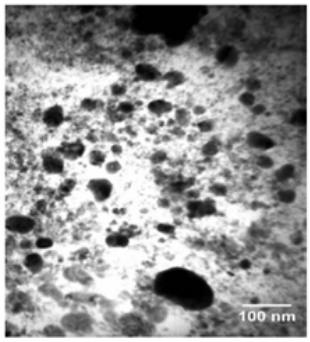

Figure 3: The TEM image of PVP coated silver nano particles [15].

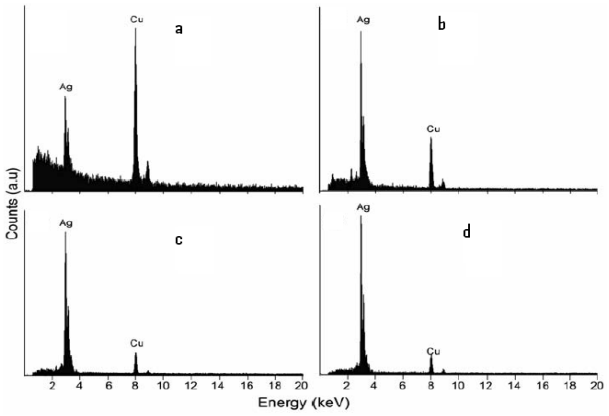

Figure 4: EDX Spectra of (a) Polymer matrix without nano particles (b) at 55 nm Size nano particles (C) at 100 nm size particles (d) at 200 nm size nano particles [15].

treated fabrics were investigated by absorption spectroscopy using a UV–Vis spectro photometer (Perkin –Elmer Lamda 35 equipped with 60mm integrating sphere). The blank reference was air. The UV profiles of untreated samples were compared with the spectra collected from the same fabrics treated with ZnO nano particles, and the effectiveness in shielding UV radiation was evaluated by measuring the UV absorption, transmission and reflection. Each measurement is the average of four scans obtained by rotating the sample by 90 °C. The transmission was used to calculate the ultraviolet protection factor (UPF) and the percent UV transmission, using the following equations.

$$UPF = \int_{\lambda_1}^{\lambda_2} E(\lambda)S(\lambda)*d\lambda \Big/ \int_{\lambda_1}^{\lambda_2} E(\lambda)S(\lambda)*Td(\lambda) \quad (1)$$

$$UV\ trasmission\ (\%) = \sum_{\lambda_1}^{\lambda_2} T(\lambda) \Big/ \lambda_2 - \lambda_1 \quad (2)$$

Where E(λ) is the relative erythemal spectral effectiveness ; S(λ), the solar spectral irradiance in W m^{-2} nm^{-1}; and T(λ), the spectral transmission of the specimen obtained from UV spectrophometric experiments. The values of E(λ) and S(λ) were obtained from the national Oceanic and Atmospheric Administration database (NOAA). The UPF values were calculated both for UV-A (315-400 nm) and for UV-B (295-315 nm). The percent UV transmission, obtained from equation (2), was determined for UV-A and UV-B radiations from the transmission spectra of the fabric samples.

Physical and Physico-chemical characterization

FTIR spectroscopy [29,30] has been used to evaluate the chemical composition of synthesized ZnO nano particles. X ray diffraction has been used to determine the crystallinity of nano particles. Dried ZnO nano particles weighing 0.5 grams has been deposited as randomly oriented powder onto a plexiglass sample container, and XRD pattern were recorded between 20° and 80° angles, with a scan rate of 1.5° per minute. The crystallite domain diameter (D) was obtained from XRD peaks using the Scherrer's equation

$$D=0.89 * \lambda / \Delta W * \cos\theta$$

Where λ is the wavelength of incident X-ray beam; θ the Bragg's diffraction angle; and ΔW the width of the X-ray pattern line at half-peak height in radians. TEM has been used to obtain the shape and

size of nano particles. The samples have been placed on carbon coated copper grids for TEM measurement. These samples were prepared from much diluted dispersion of particles in 2-propanol. The ZnO treated fabrics were analyzed through Scanning Electron Microscopy (SEM). The samples were previously coated with a thin layer of gold deposited sputtering under vacuum.

FTIR and XRD studies

Fourier Transform Infra Red (FTIR) spectroscopy is a technique which is used to obtain an infra red spectrum of absorption, emission, photoconductivity or Raman Scattering of a solid, liquid or gas. An FTIR spectrometer simultaneously collects spectral data in a wide spectral range. This confers a significant advantage over a dispersive spectrometer which measures intensity over a narrow range of wavelengths at a time. The FTIR spectra of the synthesized zinc oxide nano materials are shown in Figure 5. The spectrum relating to the first method of synthesis can be observed to be in the absorption band near 430 cm^{-1}. The peaks observed at 3450 and 2350 cm^{-1} show that C=O and –OH residues are present, which could be attributed to carbon dioxide and atmospheric moisture respectively. The same spectrum has also been obtained from the zinc oxide nano material obtained from the second method of synthesis. The images of the nano particles obtained from Transmission Electron Microscope (TEM) are shown in Figure 6. It can be seen that the nano particles are almost spherical and somewhat mono dispersed [31]. However, some larger aggregates are present in the treated fabric, as obtained from the first method of synthesis (Figure 6a). This is due to the high surface energy of the zinc oxide nano particles, which cause the aggregation, particularly when the synthesis of the nano particle is done under aqueous medium [32]. The nano particles obtained from the second method of synthesis are more mono dispersed and isolated than those obtained from the first method of synthesis. Thus the second method of synthesis gives a greater peptization than that of the first one. From Figure 6b, it can be seen that some halos envelope the nano particles owing to the retention of some diol that remains adsorbed on the ZnO nano particles, and produces tiny peaks at 2850- 2920 cm^{-1} in the FTIR spectrum as shown in Figure 5b.

X-rays are electromagnetic radiation similar to light but with a much shorter wavelength. They are produced when electrically charged particles of sufficient energy are decelerated. In an X-ray tube, the high voltage maintained across the electrodes draws electrons towards a metal target (the anode). X ray pre produced at the point of impact, and radiate in all directions

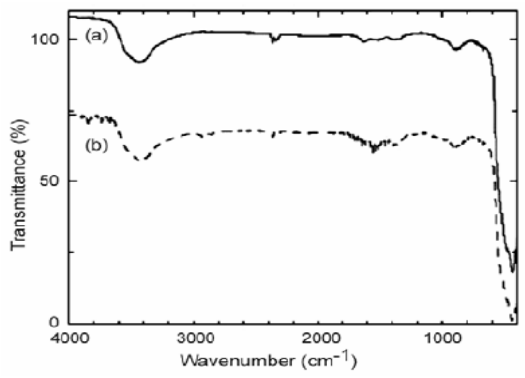

Figure 5: FTIR Spectrum of ZnO nano particles obtained from (a) synthesis 1 and (b) Synthesis 2 [32].

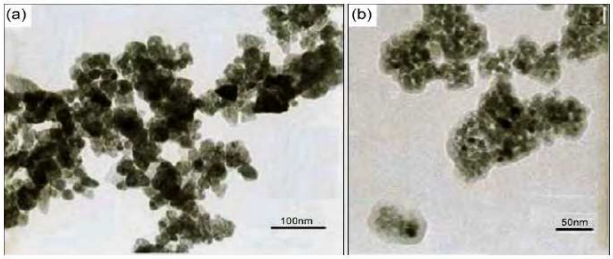

Figure 6: TEM micrographs of the materials obtained from (a) synthesis 1 and (b) synthesis 2 after three peptizations [32].

If an incident X ray beam encounters a crystal lattice, general scattering occurs although most scattering interferes with itself and is eliminated (destructive inference), diffraction occurs when scattering in a certain direction is in phase with scattered rays from other atomic planes. Under this condition the reflections combine to form new enhanced wave fronts that mutually reinforce each other (constructive inference). The relation by which diffraction occurs is known as the Bragg's law or equation. As each crystalline material including the semi crystalline polymers as well as metal and metal oxide nanoparticles and layered silicate nanoclays have a characteristic atomic structure, it will diffract X rays in a unique characteristic diffraction order or pattern.

X ray diffraction data form polymers generally provide information about crystallinity, crystallite size, orientation of the crystallites and phase composition in semi crystalline polymers. With appropriate accessories, X-ray diffraction instrumentation can be used to study the phase change as a function of stress or temperature, to determine lattice strain, to measure the crystalline modulus, and with the aid of molecular modeling to determine the structure of polymer.

Besides the above mentioned characterization this sophisticated technique can also be used to characterize polymer-layered silicate (clay) nanocomposites. Polymer / layered silicate nanoclay composites have attracted great interest, both in industry and in academia, because theyoften exhibit remarkable improvement in materials properties at very low clay content (3-6 wt%) when compared with virgin polymer or conventional composites. The use of organoclays as precursors to nanocomposite formation has been extended into various polymer systems (thermoset and thermoplastic) including epoxy and others.

For true nano composites, the clay nanolayers must be uniformly dispersed and exfoliated in the polymer matrix. The structure of polymer / layered silicates composites has typically been established using wide angle X-ray Diffraction (WAXD) analysis. By monitoring the position shape and intensityof the basal reflections from the distributed silicate layers, the nanocomposite structures (intercalated or exfoliated) may be identified. In an exfoliated nanocomposite, the extensive layer separation associated with the delamination of the original silicate layers in the polymer matrix results in the eventual disappearance of any coherent X ray diffraction from the distributed silicate layers. On the other hand, for intercalated nano composites, the finite layer expansion associated with the polymer intercalation results in the appearance of a new basal reflection corresponding to the larger gallery height.

Organophilic clay (also known as nanoclay) can be obtained by

simply the ion exchange reaction of the hydrophilic clay with an organic cation such as an alkyl ammonium or phosphonium ion to make it compatible with polymeric matrix. The inorganic ions, relatively small (sodium) re exchanged with more voluminous organic onium ions. This ion exchange reaction results in widening the gap between the single sheets, enabling organic cations chain to move in between them. This increase in d-space or degree of exfoliation of the polymer nanocomposites can be obtained from Bragg's equation. This X-ray diffractograms of the organoclay reveals a shift in the position of [001] planes (2θ changed from 5.7° to 4.32°) indicating an increase in the basal spacing of these planes. The increase is relatively large from 1.5nm to 2.06nm and confirms the occurrence of organic molecule intercalation between silicate platelets.

The X-ray diffraction spectra of the zinc oxide nano materials can be seen in Figure 7. The spectra exhibit well defined peaks typical of zinc oxide in the crystal structure of zincite. This indicates crystallinity of synthesized solids. The effects of the particle size cause broadening of the peaks in the X-ray diffraction pattern of solids. The mean crystallite size of a powder sample has been estimated from the full width at half maximum of the diffraction peak (ΔW) according to the Scherrer's equation. The values of ΔW for the first and second methods of synthesis are 0.0087 and 0.017 radians respectively. Thus using the Scherrer's equation, the average sizes of the nano particles synthesized by the first and second methods of synthesis are 20+5 nm and 10+1 nm respectively [33-35]. The important feature of the x-ray diffraction patterns is that the peaks from the second method of synthesis (Figure 7b) are broader than the peaks from the first method of synthesis (Figure 7a). This result suggests that the particles obtained from the second method of synthesis are smaller than the particles obtained from the first method of synthesis as confirmed by TEM micrographs (Figure 6), and reflects the effects due to the experimental conditions on the nucleation and growth of the crystal nuclei. The morphology and size of the nano particles are greatly influenced by the experimental conditions. Interestingly when the reaction temperature in water is raised from 90 °C, to that in 1,2-ethanediol, to 150 °C, the nano particle size gets reduced from 20 to 9 nm.

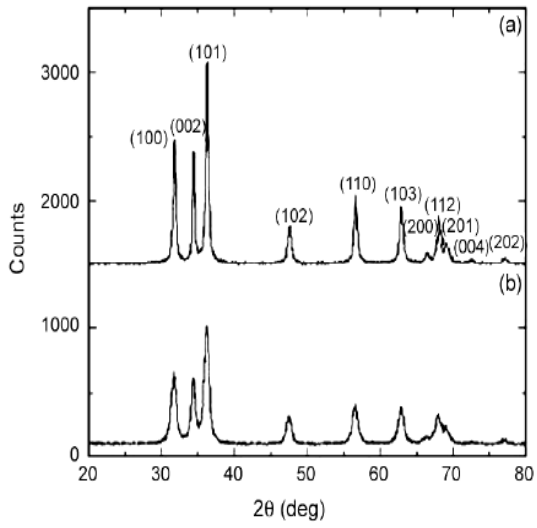

Figure 7: XRD patterns of the material obtained from (a) Synthesis 1 and (b) Synthesis 2 [32].

Electron Microscopy

The Scanning Electron Microscope (SEM) is an electron microscope that images the sample surface by scanning it with a high energy beam of electrons. Conventional light microscopes use a series of glass lenses to bend light waves and create a magnified image while the scanning electron microscope creates the magnified images by using electrons instead of light waves [2]. When the beam of electrons strikes the surface of the specimen and interacts with the atoms of the sample, signals in the form of secondary electrons, back scattered electrons and characteristic X-rays are generated that contain information about the sample's surface topography, composition, etc. The SEM can produce very high-resolution images of a sample surface, revealing details about 1-5 nm in size in its primary detection mode i.e. secondary electron imaging. Characteristic X-rays are the second most common imaging mode for an SEM. These characteristic X-rays are used to identify the elemental composition of the sample by a technique known as energy dispersive X-ray (EDX). Back-scattered electrons (BSE) that come from the sample may also be used to form an image. BSE images are often used in analytical SEM along with the spectra made from the characteristic X-rays as clues to the elemental composition of the sample.

In a typical SEM, the beam passes through pairs of scanning coils or pairs of deflector plates in the electron column to the final lens, which deflect the beam horizontally and vertically so that it scans in a raster fashion over a rectangular area of the sample surface. Electronic devices are used to detect and amplify the signals and display them as an image on a cathode ray tube in which the raster scanning is synchronized with that of the microscope. The image displayed is therefore a distribution map of the intensity of the signal being emitted from the scanned area of the specimen.

SEM requires that the specimens should be conductive for the electron beam to scan the surface and that the electrons have a path to ground for conventional imaging. Non-conductive solid specimens are generally coated with a layer of conductive material by low vacuum sputter coating or high vacuum evaporation. This is done to prevent the accumulation of static electric charge on the specimen during electron irradiation. Non-conducting specimens may also be imaged uncoated using specialized SEM instrumentation such as the "Environmental SEM" (ESEM) or in field emission gun (FEG) SEM operated at low voltage, high vacuum or at low vacuum, high voltage.

The SEM shows very detailed three dimensional images at much high magnifications (up to ×300000) as compared to light microscope (up to × 10000). But as the images are created without light waves, they are black and white. The surface structure of polymer nano composites, fracture surfaces, nano fibres, nanoparticles and nanocoating can be imaged through SEM with great clarity. As very high resolution images of the dimensions 1-5 nm can be obtained, SEM is the most suitable process to study the nano fibres and nano coatings on polymeric/textile substrate.

Electro spun nano fibres are extensively studied in biomedical, environmental and other technical textile applications for their high surface area. Electrospun nylon 6 nano fibres decorated with surface bound silver nano particles used for anti bacterial air purifier can be categorized using SEM (Figure 8a). In tissue engineering or cell culture applications, the SEM image is the prime characterization

technique for scaffold construction, cell development and growth (Figure 8b). SEM technique (Figure 8c) is used to observe the plied CNT yarns in 3D braided structures.

The SEM technique can also be used to view dispersion of nano particles such as carbon nano tubes, nano clays and hybrid POSS nano fillers in the bulk and on the surface of nano composite fibres and coatings on yarns and fabric samples.

SEM has been used for examination of the treated fabric surface [2]. Figure 9a shows the nano scaled zinc oxide nano particles as seen on polyester/cotton fabrics. The nano particles are well dispersed on the fibre surface in both the cases, although some aggregated nano particles are still visible [31].

The particle size plays a primary role in determining their adhesion to the fibres. The largest particle agglomerates can get easily removed from the fibre surface, while the smaller particles will penetrate deeper and adhere strongly into the fibre matrix. The SEM image in Figure 9b confirms that most of the large agglomerates are removed from the textile surface after washing.

Characterization of Titanium Dioxide Nano Particles

Characterization of nano particles was done by three tests such as X-ray Diffraction method and Fourier Transform infrared spectroscopy (FTIR) and transmission of electron microscope [34]. The crystallinity was determined by XRD using a Bruker D8 advance X ray diffractrometer equipped with a CuKa (λ=1.54 A°) source (applied voltage 40 kV, current 40 mV). About 0.5 gram of the dried particles were deposited as a randomly oriented powder onto a Plexiglas sample container, and the XRD patterns were recorded at angles between 20° and 80° with a scan rate of 1.5° per min.

The crystalline domain diameters (D) were obtained from XRD peaks according to the scherer's equation:

$$D = \frac{0.89\lambda}{\Delta W \ Cos\theta}$$

Where λ is the wave length of the incident X0ray beam (1.54 Å for CuKa), θ is the Bragg's diffraction angle, ΔW is the width of the X-ray pattern line at half peak height in radians. The chemical composition of synthesized materials was checked by FTIR spectroscopy with a Bio-Rad FTS-40 spectrometer. The shape and size of the nano particles were obtained through TEM using a Philips EM201C apparatus operating at 80 kv. The samples for TEM measurement were prepared from much diluted dispersion of the particles in 2-propanol. Surface area measurement was determined from BET on a coulter SA 3100 surface area analyzer, under N2 flow.

Characterization of Silica Nano Particles

Colloidal silica nano-particles are based on the hydrolysis

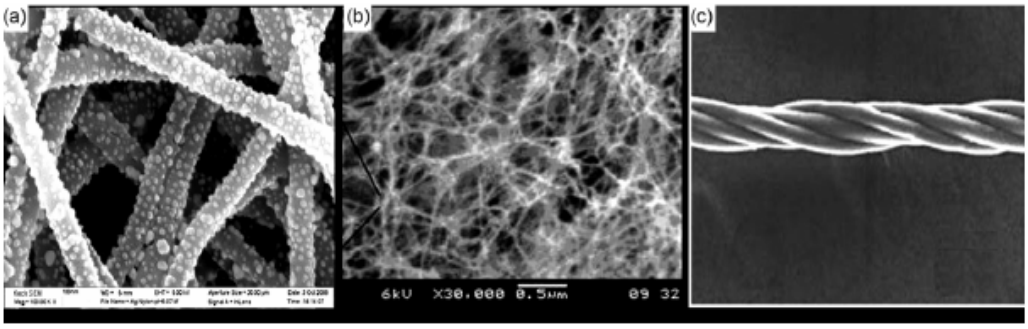

Figure 8: (a) Electrospun nylon 6 nano fibres with surface bound silver nano particles,
(b) Peptide nano fibre scaffold for tissue engineering, and
(c) SEM image of plied CNT yarn [1].

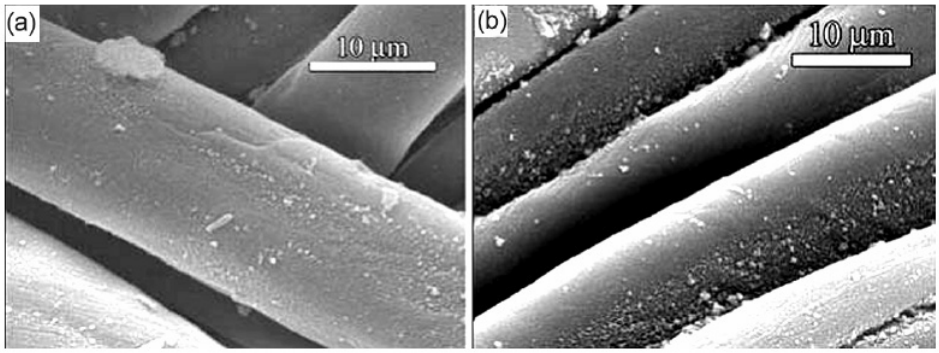

Figure 9: SEM images of ZnO nano particles obtained from synthesis 1 on (a) Polyester/Cotton before washing and (b) Cotton after washing [31].

reaction of silicon alkoxide where the resulting particle size and morphology depend strongly on the hydrolysis kinetics. In the selected constituent concentrations, spherical, silica particles can be obtained. The reaction time of this synthesis required 15 minutes. The reaction continues until the solution is super-saturated [35]. To investigate the possibility of tailoring the particle size and maybe the particle size distribution, a kinetic study of the particle size evolution as a function of reaction time was carried out. X-ray diffraction using CuKα radiation (Philips X'pert) was used to determine the crystalline structure of silica particles [36]. The silica particles were amorphous according to XRD with peaks less than $2\theta=10^{o}$ conforming to the JCPDS file (79-1711). This demonstrates that a high percentage of these particles are amorphous, but a few of them are crystalline, as the energy of amorphous silica is very close to that of crystalline silica [37]. It has been reported that when one is interested in fine particles, the water concentrations should be fixed at 0.2-3.2 M, also the molar ratio of ammonia and TEOS should be the same. Silica nano-particles were prepared taking into account these considerations. Figure 10 shows these particles and also the narrow size distribution of these particles [38].

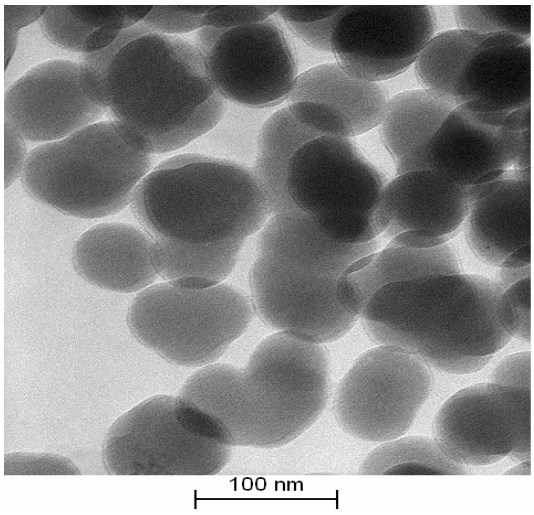

Figure 10: TEM image of silica nano particles [39].

Vasconcelos and Campos [39] have considered the effect of different molar ratios of reagents on the structure and morphology of silica particles at room temperature. When the reaction was conducted at 60°C, silica nano-particles were also obtained. This temperature was based upon a limitation of the boiling point of the reagents.

Figures 10 and 11 show spherical and agglomerated silica nano-particles, which were obtained using different molar ratios of reagents; the molar ratio of the solvent is also important. With a lower molar ratio of solvent (ethanol), agglomerated silica particles were obtained. Park and Kim [40] have shown when a narrow size distortion is required; a small molar ratio of ethanol should be employed.

The optimum conditions for synthesizing silica nano-particles were considered to be with the same molar ratio of TEOS and ammonia and a higher molar ratio of ethanol giving rise to smaller silica nanoparticles with a broad distribution of particle sizes [41]. Stober and Fink [42] have shown the different solvent effects on the size of particles. Using different solvents such as methanol, ethanol, propanol, butanol and ethanol-glycerol, different structures were obtained. From methanol and ethanol-glycerol, a stable sol could be obtained, but when butanol and ethanol were used, precipitation could be easily observed. Different experiments show that the presence of glycerol during synthesis affects the precipitation [37].

Conclusion

The various nano materials used in textile finishing have been characterized by the use of the Scanning Electron Microscope, Infra Red Spectroscopy, Tunneling Electron Microscopy, and X-ray Diffraction techniques. The nano particles observed were silver oxide, titanium dioxide, and zinc oxide, which are considered to be very important in the textile finishing process.

The studies enable to determine the nano particle size, the surface characteristics of the fabrics on which they have been applied. The chemical composition of the nano materials has also been determined.

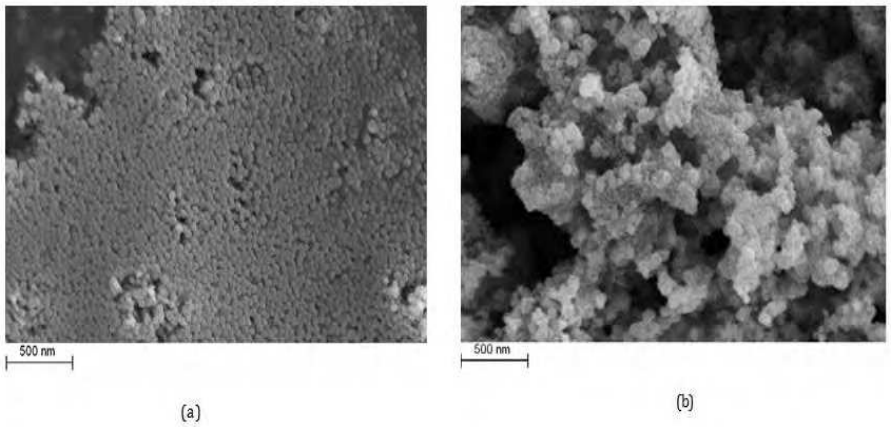

Figure 11: SEM micrographs of silica particles obtained from a molar ratio of water:TEOS:Ammonia:Ethanol [(a) 1:4:6:6 (b) 1:4:6:24].

Table 1: The scope of the various characterization techniques

S.No	Types of Characterization techniques	Areas of applications
1	Scanning electron microscopy	Surface structures of nano particles, dispersion of nano particles, and surface of coated fibers and fabrics
2	Energy dispersive X-ray analysis	Composition or the amount of nanoparticles near and at the surface can be estimated, provided, they contain some heavy metal ions. Suited for silver nano particles
3	Transmission electron microscopy	Enable to reveal the distribution of nano particles in polymer matrices of nano composite fibers, nanocoatings etc. The extent of exfoliation, intercalation and orientation of nanoparticles can also be visualized.
4	High resolution transmission electron microscopy	Enables study of nanoscale properties of nano materials. At such a high resolution, individual atoms and crystalline defects can be imaged.
5	Atomic force microscope	Important in fundamental and practical research and development of versatile technical textiles for a variety of applications. Also suggests possible ways to investigate the effect of plasma processing on the morphology of textile surfaces
6	Scanning tunneling microscopy	A powerful tool in nanotechnology and nanoscience providing facilities for characterization and modification of a variety of materials. It can move metal atoms and molecules on smooth surfaces with high precision.
7	Raman spectroscopy	Applicable for raman active textile fibers such as aramid and carbon

FTIR spectroscopy has enabled to identify the chemical composition of synthesized nano particles. X-ray diffraction studies have helped in determination of the crystallinity of nano particles. The Table 1 gives the scope of the various characterization techniques.

References

1. Joshi M, Bhattacharya A, Wazed Ali (2008) Characterization techniques for nanotechnology applications in textiles. IJFTR 33: 304-317.
2. Scanning Electron Microscope, Radiological and Environmental Management (REM). Purdue University.
3. Mills K, Dong H, Nano fibre technology: Introduction to production and treatment. Cornell University, New York, USA.
4. Zhang S, Gelain F, Zhao X (2005) Designer self-assembling peptide nanofiber scaffolds for 3D tissue cell cultures. Seminars in cancer Biology 15: 413-420.
5. Bradford PD, Bogdanovich AE (2008) Electrical Conductivity Study of Carbon Nanotube Yarns, 3-D Hybrid Braids and their Composites. Journal of Composite Materials 42: 1533-1545.
6. Joshi V, Vishwanathan V (2006) High-performance filaments from compatibilized polypropylene/clay nanocomposites. J Appl Polym Sci 102: 2164-2174.
7. Joshi M, Butola BS, Simon G, Kulalevab N (2006) Rheological and Viscoelastic Behavior of HDPE/Octamethyl-POSS Nanocomposites. Macromolecules 39: 1839-1849.
8. Yeo MK, Kang M (2008) Effects of Nanometer Sized Silver Materials on Biological Toxicity During Zebrafish Embryogenesis. Bulletin of Korean Chemical Society, 29: 1179-1184.
9. Reddy NP, Pena-Mendez EM, Havel J (2008) Silver or silver nanoparticles: a hazardous threat to the environment and human health. J Appl Biomed 6: 117-129.
10. Ma J, Qi Z, Hu Y (2001) Synthesis and characterization of polypropylene/clay nanocomposties. J Appl Polm Sci 82: 3611-3617.
11. Pal S, Tak YK, Song JM (2007) Does the Antibacterial Activity of Silver Nanoparticles Depend on the Shape of the Nanoparticle? A Study of the Gram-Negative Bacterium Escherichia coli. Appl Environ Microbiol 73: 1712-1720.
12. Brause RH, Moeltgen, Kleinermanns K (2002) Characterization of laser-ablated and chemically reduced silver colloids in aqueous solution by UV/VIS spectroscopy and STM/SEM microscopy. Appl Phys B 75: 711-716.
13. Mulvaney P (1996) Surface Plasmon Spectroscopy of Nanosized Metal Particles. Langmuir 12: 788-800.
14. Mie G (1908) Beiträge zur Optik trüber Medien, speziell kolloidaler Metallösungen. Ann Phys 330: 377-445.
15. Raja ASM, Thilagavathi G, Kannaiyan T (2010) Synthesis of spray dried polyvinyl pyrrolidone coated silver nano powder and its application on wool and cotton for microbial resistance. IJFTR 10: 59-64.
16. Ma J, Ai Z, Hu Y (2001) Synthesis and characterization of polypropylene/clay nanocomposties. J Appl Polym Sci 82: 3611-3617.
17. Klajn R, Bishop KJM, Fialkowski M, Paszewski M, Campbell CJ, et al. (2007) Plastic and Moldable Metals by Self-Assembly of Sticky Nanoparticle Aggregates. Science 316: 261-264.
18. Marcato PD, De Souza G, Alves OL, Esposito E, Duran N (2005) Antibacterial activity of silver nanoparticles synthesized by fusarium oxysporum strain.
19. Vighneswaran N, Kumar S, Kathe AA, Varadarajan PV, Prasad V (2006) Functional finishing of cotton fabrics using zinc oxide soluble-starch nano composites. Nanotechnology 17: 5087-5095.
20. Qi K, Chen X, Liu Y, Xin JH, Mak CL, et al. (2007) Facile preparation of anatase/SiO2 spherical nano composites and their application in self cleaning textiles. J Mater Chem 17: 3504-3508.
21. Baglioni P, Dei L, Fratoni L, Lo Nostro P, Moroni M (2003) Preparation of nano and microparticles of group II and transition metals, oxides and hydroxides and their use in the ceramic, textile and paper industries. WO Patent 2003082742.
22. Pan ZW, Dai ZR, Wang ZL (2001) Nanobelts of semiconducting oxides. Science 291: 1947-1949.
23. Arnold MS, Avouris P, Pan ZW, Wang ZL (2003) Field effect transistors based on semiconducting oxide nano belts. J Physl Chem B 107: 659-663.
24. Sawai J (2003) Quantitative evaluation of antibacterial activities of metallic oxide powders (ZnO, MgO and CaO) by conductimetric assay. J Microbiol Methods 54: 177-182.
25. Xiong M, Gu G, You B, Wu L (2003) Preparation and characterization of poly(styrene butylacrylate) latex/ZnO nano composites. J Appl Polym Sci 90: 1923-1931.
26. Behnajady MA, Modirshahla N, Hamzavi R (2006) Kinetic study on photocatalytic degradation of CI acid yellow 23 by ZnO photocatalyst. J Hazard Mater 133: 226-232.
27. Tang E, Cheng G, Ma X, Pang X, Zhao Q (2006) Surface modification of zinc oxide nano particle by PMMA and its dispersion in aqueous system. Appl Surf Sci 252: 5227-5232.
28. Tang E, Cheng G, Ma X (2006) Preparation of Nano-ZnO/PMMA composite particles via grafting of the copolymer onto the surface of zinc oxide particles. Powder Technol 161: 209-214.
29. Hačko J, Andrić S, Ražić SE (2011) Funcionality of textiles using plasma. Scientific book: Young scientist in the protective textile research, TSRC.
30. Paul G, Paul W (2003) Identification of cellulosic fibres by FTIR spectroscopy: Thread and single fibre analysis by attenuated total reflectance. Studies in Conservation 48: 269-275.
31. Kathirvelu S, D'Souza L, Dhurai B (2009) UV protection finishing of textiles using ZnO nano particles. IJFTR 34: 267-273.
32. Becheri A, Dürr B, Lo Nostro P, Baglioni P (2008) Synthesis and Characterization of zinc oxide nano particles: Application to textiles as UV absorbers. J Nanopart Res 10: 679-689.

33. Parthasarathi V, and Thilagavathi G, Synthesis and characterization of titanium dioxide nanoparticles and their applications to textiles for microbe resistance. JTATM 6: 1-8.

34. Ray S, Okamoto M (2003) Polymer/layered silicate nanocomposites: a review from preparation to processing. Prog Polym Sci 28: 1539-1641.

35. Griffiths P, de Hasseth JA (2007) Fourier Transform Infrared Spectrometry (2nd edtn), John Wiley & Sons, USA.

36. Her YS, Lee SH, Matijević E (1996) Continuous precipitation of monodispersed colloidal particles. II. SiO2, Al(OH)3, and BaTiO3. Journal of Materials Research 11: 156-161.

37. Tabatabaei S, Shukhohfar A, Aghababazadeh R, Mirhabibi A (2006) Experimental study of the synthesis and characterization of silica nanoparticles via the sol gel method. J Phys: Conf Ser 26: 371-374.

38. Kolbe G (1956) Das Komplexchemische Verhalten der Kieselsaure. Dissertation, Friedrich- Schiller University Jena.

39. Vasconcelos DCL, Campos WR, Vasconcelos V, Vasconcelos WL (2002) Influence of process parameters on the morphological evolution and fractal dimension of sol–gel colloidal silica particles. Material Science and Engineering A 334: 53-58.

40. Park SK, Kim KD (2002) Preparation of silica nanoparticles: determination of the optimal synthesis conditions for small and uniform particles. Colloid Surface A 197: 7-17

41. Van Blaaderen A, Vrij A (1993) Synthesis and Characterization of Monodisperse Colloidal Organo-silica Spheres. J Colloid Interf Sci156: 1-18.

42. Stober W, Fink A (1968) Controlled growth of monodisperse silica spheres in the micron size range. J Colloid Interf Sci 26: 62-69.

Author Affiliations

Top

NIFT TEA College of Knitwear Fashion, Tirupur 641 606, India